OPEN ACCESS
Fractals, Vol. 31, No. 10 (2023) 2340005 (20 pages)
© The Author(s)
DOI: 10.1142/S0218348X23400054

World Scientific
www.worldscientific.com

Fractals 2023.31. Downloaded from www.worldscientific.com
by CANKAYA UNIVERSITY on 06/04/24. Re-use and distribution is strictly not permitted, except for Open Access articles.

IMPACT OF PUBLIC HEALTH AWARENESS PROGRAMS ON COVID-19 DYNAMICS: A FRACTIONAL MODELING APPROACH

ZAIN UL ABADIN ZAFAR,[*] ABDULLAHI YUSUF,[†,‡] SALIHU S. MUSA,[§,¶]
SANIA QURESHI,[‖,**,††,***,‡‡‡] ALI S. ALSHOMRANI[‡‡]
and DUMITRU BALEANU[§§,¶¶,‖‖,†††,‡‡‡]

[*]*Department of Mathematics*
Faculty of Sciences and Technology
University of Central Punjab, Lahore, Pakistan

[†]*Department of Computer Engineering*
Biruni University, Istanbul, Turkey

[‡]*Department of Mathematics, Science Faculty*
Federal University Dutse, Jigawa, Nigeria

[§]*Department of Applied Mathematics*
Hong Kong Polytechnic University, Hong Kong

[¶]*Department of Mathematics*
Kano University of Science and Technology
Wudil, Nigeria

[‖]*Department of Basic Sciences and Related Studies*
Mehran University of Engineering and Technology
Jamshoro 76062, Pakistan

[**]*Department of Computer Science and Mathematics*
Lebanese American University, Beirut
P. O. Box 13-5053, Lebanon

[‡‡‡]Corresponding authors.

This is an Open Access article in the "Special Issue on Fractal AI-Based Analyses and Applications to Complex Systems: Part IV", edited by Yeliz Karaca (University of Massachusetts Chan Medical School, USA), Dumitru Baleanu (Cankaya University, Turkey & Institute of Space Sciences, Romania), Majaz Moonis (University of Massachusetts Chan Medical School, USA), Yu-Dong Zhang (University of Leicester, Leicester, UK) & Osvaldo Gervasi (Perugia University, Perugia, Italy) published by World Scientific Publishing Company. It is distributed under the terms of the Creative Commons Attribution 4.0 (CC BY) License which permits use, distribution and reproduction in any medium, provided the original work is properly cited.

[††]Department of Mathematics
Near East University, 99138 Mersin, Turkey
[‡‡]Department of Mathematics
King Abdulaziz University, Jeddah, Saudi Arabia
[§§]Department of Mathematics, Çankaya University
Öğretmenler Cad. 1406530, Ankara, Turkey
[¶¶]Institute of Space Sciences
Măgurele, Bucharest, Romania
[‖‖]Department of Medical Research
China Medical University Hospital
China Medical University, Taichung, Taiwan
[***]sania.qureshi@faculty.muet.edu.pk
[†††]dumitru@cankaya.edu.tr

Received January 17, 2022
Accepted September 24, 2022
Published September 12, 2023

Fractals 2023.31. Downloaded from www.worldscientific.com
by CANKAYA UNIVERSITY on 06/04/24. Re-use and distribution is strictly not permitted, except for Open Access articles.

Abstract

Public health awareness programs have been a crucial strategy in mitigating the spread of emerging and re-emerging infectious disease outbreaks of public health significance such as COVID-19. This study adopts an Susceptible–Exposed–Infected–Recovered (SEIR) based model to assess the impact of public health awareness programs in mitigating the extent of the COVID-19 pandemic. The proposed model, which incorporates public health awareness programs, uses ABC fractional operator approach to study and analyze the transmission dynamics of SARS-CoV-2. It is possible to completely understand the dynamics of the model's features because of the memory effect and hereditary qualities that exist in the fractional version. The fixed point theorem has been used to prove the presence of a unique solution, as well as the stability analysis of the model. The nonlinear least-squares method is used to estimate the parameters of the model based on the daily cumulative cases of the COVID-19 pandemic in Nigeria from March 29 to June 12, 2020. Through the use of simulations, the model's best-suited parameters and the optimal ABC fractional-order parameter τ may be determined and optimized. The suggested model is proved to understand the virus's dynamical behavior better than the integer-order version. In addition, numerous numerical simulations are run using an efficient numerical approach to provide further insight into the model's features.

Keywords: Fractional; Optimal ABC; Boxplot; Least-Squares; Existence; Uniqueness.

1. INTRODUCTION

COVID-19, a disease caused by SARS-CoV-2, is a life-threatening respiratory pathogen that emerged in Wuhan, China[1–3] and later spread to all parts of the world to become the first pandemic caused by the coronavirus family.[4] As of September 1, 2021, it was reported that the disease had affected >217 million, including >4.5 million mortality worldwide. Public awareness is a crucial control measure to prevent and curtail the spread of emerging and re-emerging infectious diseases, including the current COVID-19 pandemic.[5] Public health awareness programs have been implemented in many countries across the globe to mitigate SARS-CoV-2 infection.

Fractals 2023.31. Downloaded from www.worldscientific.com
by CANKAYA UNIVERSITY on 06/04/24. Re-use and distribution is strictly not permitted, except for Open Access articles.

Proper implementation and well-planed non-pharmaceutical interventions (NPIs) measures remain the most effective strategy in controlling the distribution of SARS-CoV-2,[6,7] despite the increasing rate of vaccination (over 5.2 billions doses of vaccine have been administered by September 1, 2021).[8] Many countries have succeeded in suppressing the number of active cases and deaths due to the high compliance of NPIs by the general public, which is directly proportional to the rate at which the population becomes aware of the disease and the implications it might cause due to noncompliance with NPIs.[9,10]

There is a need to increase public health education programs/campaigns worldwide to continue suppressing the morbidity and mortality of COVID-19. This is because even in some developed countries such as the US and UK, some people still believe in conspiracy theories and rumors regarding the COVID-19 pandemic or the implication of vaccination, which causes an increase in noncompliance of NPIs measures, indicating that the general public needs more enlightenment/awareness on the impact of SARS-CoV-2 in order to convince them to comply with public health policies properly.

Implementing proper public health awareness programs coupled with other NPIs measures can effectively change public perspectives on the infection risk and severity of SARS-CoV-2. It could help to educate individuals to make necessary changes to their routine behavior to reduce the exposure to the causative agent, and the possibility of infection. Public health awareness programs can be implemented physically with the help of health professionals; via news media such as posters, newspapers, fliers, television, and radio advertisements; or through social media such Twitter, Facebook, LinkedIn, WeChat with the common aim of dissemination of information to the general public about the disease severity and direct them toward appropriate prevention and intervention during the epidemic. Increasing the rate of awareness programs for the COVID-19 pandemic would be especially useful in developing countries where people have limited access to the internet and social media that have been increasingly common in developed countries as the leading source for information update.[11]

A lot of epidemiological modeling studies have been done recently to shed light and understanding on the spread of SARS-CoV-2,[12,13] and provided suggestions for the most effective control measures.[14] Some reports also assessed the impact of NPIs measures on reducing the parthenogenesis of SARS-CoV-2, ascertained effectiveness of the vaccines,[15] determined the spatiotemporal variability and heterogeneous severity of SARS-CoV-2,[16] estimation of generation interval, attack rate, and infection fatality rate.[17,18]

As can be seen from the preceding facts, the COVID-19 infection is a major and devastating health condition that affects people from all walks of life; hence quantitative analysis of the disease is critical for the literature. Using a fractional modeling technique, we investigated the influence of public health awareness campaigns on lowering COVID-19 parthenogenesis in this study. We recommend the reader to Ref. 19 for the traditional form of the proposed model. The ABC fractional operator is one of the most important operators in the application, although there are many different fractional derivatives and integral operators in fractional calculus.[20] As a result, we observe and interpret how the arbitrarily chosen fractional-order affects the model's behavior by analyzing it theoretically and numerically with the ABC differential operator. We refer the reader to a number of epidemiological models that have been examined using different forms of fractional derivatives[21–28] including ABC while justifying its use in the modeling of infectious diseases such as COVID-19.

2. MODEL DESCRIPTION

The model in classical sense has been designed in the following form:

$$\begin{cases} \dfrac{\mathrm{d}S_a}{\mathrm{d}t} = -\dfrac{a_1 a_2 S_a}{N}(a_3 A + I) + a_4 S_u, \\ \dfrac{\mathrm{d}S_u}{\mathrm{d}t} = -\dfrac{a_2 S_u}{N}(a_3 A + I) - a_4 S_u, \\ \dfrac{\mathrm{d}E}{\mathrm{d}t} = \dfrac{a_2}{N}(a_3 A + I)(a_1 S_a + S_u) - a_5 E, \\ \dfrac{\mathrm{d}A}{\mathrm{d}t} = a_6 a_5 E - a_7 A, \\ \dfrac{\mathrm{d}I}{\mathrm{d}t} = (1 - a_6) a_5 E - (a_8 + a_9 + a_{10} + a_{11}) I, \\ \dfrac{\mathrm{d}H_m}{\mathrm{d}t} = a_9 I + a_{12} H_s - (a_3 + a_{14}) H_m, \\ \dfrac{\mathrm{d}H_s}{\mathrm{d}t} = a_{10} I + a_{14} H_m - (a_{15} + a_{12} + a_{16}) H_s, \end{cases}$$

Fractals 2023.31. Downloaded from www.worldscientific.com
by CANKAYA UNIVERSITY on 06/04/24. Re-use and distribution is strictly not permitted, except for Open Access articles.

$$\begin{cases} \dfrac{\mathrm{d}R}{\mathrm{d}t} = a_7A + a_8I + a_{13}H_m + a_{15}H_s, \\ \dfrac{\mathrm{d}D}{\mathrm{d}t} = a_{11}I + a_{16}H_s. \end{cases} \tag{1}$$

The term $\frac{a_2(a_3A+I)}{N}$ represents the force of infection of the COVID-19 model (1).

The mathematical model given in (1) has been previously examined in Ref. 19. This model, however, excludes the effects of memory, which are present in many biological systems. As a result, in order for the mathematical formulation to account for memory effects, we alter the model by substituting the standard derivative with the newly introduced ABC fractional operator. For this purpose, let us obtain the fractional representation of (1) by considering the operator ${}_0^{\mathrm{ABC}}D_t^{\tau_1}$:

$$\begin{cases} {}_0^{\mathrm{ABC}}D_t^{\tau_1} S_a(t) = -\dfrac{a_1a_2S_a}{N}(a_3A + I) + a_4S_u, \\ {}_0^{\mathrm{ABC}}D_t^{\tau_1} S_u(t) = -\dfrac{a_2S_u}{N}(a_3A + I) - a_4S_u, \\ {}_0^{\mathrm{ABC}}D_t^{\tau_1} E(t) = \dfrac{a_2}{N}(a_3A + I)(a_1S_a + S_u) - a_5E, \\ {}_0^{\mathrm{ABC}}D_t^{\tau_1} A(t) = a_6a_5E - a_7A, \\ {}_0^{\mathrm{ABC}}D_t^{\tau_1} I(t) \\ \qquad = (1 - a_6)a_5E - (a_8 + a_9 + a_{10} + a_{11})I, \\ {}_0^{\mathrm{ABC}}D_t^{\tau_1} H_m(t) = a_9I + a_{12}H_s - (a_3 + a_{14})H_m, \\ {}_0^{\mathrm{ABC}}D_t^{\tau_1} H_s(t) \\ \qquad = a_{10}I + a_{14}H_m - (a_{15} + a_{12} + a_{16})H_s, \\ {}_0^{\mathrm{ABC}}D_t^{\tau_1} R(t) = a_7A + a_8I + a_{13}H_m + a_{15}H_s, \\ {}_0^{\mathrm{ABC}}D_t^{\tau_1} D(t) = a_{11}I + a_{16}H_s, \end{cases} \tag{2}$$

where $0 < t \le T$ and ${}_0^{\mathrm{ABC}}D_t^{\tau}$ denotes the AB operator in Caputo's sense of order $\tau \in 0 < t \le 1$. Based on recently conducted research study in Ref. 29, the use of a fractional operator to model infectious diseases is justified wherein one of the strongest points is the mere replacement of positive integer n in the well-known Cauchy formula for repeated integration by a positive real number $\alpha \in \mathbb{R}$ to obtain the Riemann–Liouville (RL) integral formula for the classical fractional calculus. The RL formula is the basic building block for several ground-breaking research works in the literature including numerical fractional calculus.

2.1. Preliminaries

This portion of the present work is dedicated to basic findings connected to the current investigation.

Definition 1. If we substitute $z(t) \in \mathbb{H}^1(0,T)$, then the ABC derivative ${}_0^{\mathrm{ABC}}D_t^{\tau_1}$ given by

$${}_0^{\mathrm{ABC}}D_t^{\tau_1} z(t) = \frac{Z(\tau_1)}{(1-\tau_1)} \int_0^t \frac{d}{dt} z(\rho) \times Z_{\tau_1}\left[\frac{-\tau_1(t-\rho)}{1-\tau_1}\right] d\rho. \tag{3}$$

For the Caputo–Fabrizio operator we attain $Z_{\tau_1}[\frac{-\tau_1(t-\rho)}{1-\tau_1}]$ by $e^{[\frac{-\tau_1(t-\rho)}{1-\tau_1}]}$. It should be noted that ${}_0^{\mathrm{ABC}}D_t^{\tau_1}(\text{const.}) = 0$.

Definition 2. Let $z \in L[0,T]$, then the fractional integral for the AB operator in the Caputo sense is given by

$${}_0^{\mathrm{ABC}}D_t^{\tau_1} z(t) = \frac{(1-\tau_1)}{Z(\tau_1)} z(t) + \frac{\tau_1}{Z(\tau_1)\Gamma(\tau_1)} \times \int_0^t \frac{z(\rho)}{(t-\rho)^{1-\tau_1}} d\rho. \tag{4}$$

Theorem 1. *The Atangana–Baleanu operator is given as follows:*

$${}_0^{\mathrm{ABC}}D_t^{\tau_1} z(t) = g(t)$$

has a unique solution as

$$z(t) = \frac{1-\tau_1}{Z(\tau_1)} g(t) + \frac{\tau_1}{Z(\tau_1)\Gamma(\tau_1)} \times \int_0^t \frac{g(\rho)}{(t-\rho)^{1-\tau_1}} d\rho. \tag{5}$$

Definition 3. Let

$$\begin{gathered} {}_0^{\mathrm{ABC}}D_t^{\tau_1} z(t) = g(t, z(t)), \\ z(0) = z_0 \end{gathered} \tag{6}$$

be a nonlinear fractional operator. Then the scheme for ABC operator is expressed as

$$z(t_{i+1}) = z_0 + \frac{1-\tau_1}{Z(\tau_1)} z(t_{i+1}^Q) + \frac{\tau_1 h^{\tau_1}}{Z(\tau_1)\Gamma(\tau_1)} \times \left[\sum_{j=0}^{i} a_{i+1,j} g(t_j, z(t_j)) + a_{i+1,j+1} g(t_{i+1}, z(t_{i+1}^Q))\right] \tag{7}$$

Fractals 2023.31. Downloaded from www.worldscientific.com
by CANKAYA UNIVERSITY on 06/04/24. Re-use and distribution is strictly not permitted, except for Open Access articles.

and

$$z(t_{i+1}^{Q}) = z_0 + \frac{1-\tau_1}{Z(\tau_1)} z(t_i) + \frac{h^{\tau_1}}{Z(\tau_1\Gamma(\tau_1))} \times \sum_{j=0}^{i} b_{i+1,j} g(t_j, z(t_j)), \tag{8}$$

where

$$a_{i+1,j} = \begin{cases} i^{\tau_1+1} - (i+1)^{\tau_1}(i-\tau_1) & \text{for } j = 0, \\ (i-j+2)^{\tau_1+1} - (i-j)^{\tau_1+1} & \\ \quad -2(i-j+1)^{\tau_1+1} & \text{for } 1 \le j \le i, \\ 1 \quad \text{for } j = i+1 & \end{cases} \tag{9}$$

and

$$b_{i+1,j} = -(i-j)^{\tau_1} + (i-j+1)^{\tau_1} \quad \text{for } 0 \le j \le i. \tag{10}$$

To perform qualitative study, we choose Banach space as $Z^* = \mathbb{X}_1 \times \mathbb{X}_1 \times \mathbb{X}_1 \times \mathbb{X}_1 \times \mathbb{X}_1 \times \mathbb{X}_1 \times \mathbb{X}_1 \times \mathbb{X}_1 \times \mathbb{X}_1$, where $\mathbb{X}_1 = C[0,T]$ and $\|\cdot\|$ is defined by $\mathbb{H}$ is given by $\|\mathbb{H}\| = \|(S_a, S_u, E, A, I, H_m, H_s, R, D)\| = \max_{t\in[0,T]} \|S_a + S_u + E + A + I + H_m + H_s + R + D\|$. For the proof of our results, we will use the following theorem.

Theorem 2. *For a convex subset $\mathbb{G}$ of Z^*, suppose that $\mathbb{F}, \mathbb{G}$ are two operators such as*

(i) $\Phi_1 z + \Phi_2 z \in \mathbb{G}$ *for every* $z \in \mathbb{G}$.
(ii) Φ_1 *is contraction.*
(iii) Φ_2 *is continuous and compact.*

Then the operator equation $\Phi_1 z + \Phi_2 z = z$, has minimum of one solution.

3. QUALITATIVE ANALYSIS

3.1. Existence of the ABC System

To discuss the existence of the solution of fractional-order model (2), we first define the following:

$$\begin{cases} \Theta_1(S_a,\ldots) = -\dfrac{a_1 a_2 S_a}{N}(a_3 A + I) + a_4 S_u, \\ \Theta_2(S_a,\ldots) = -\dfrac{a_2 S_u}{N}(a_3 A + I) - a_4 S_u, \\ \Theta_3(S_a,\ldots) = \dfrac{a_2}{N}(a_3 A + I)(a_1 S_a + S_u) - a_5 E, \\ \Theta_4(S_a,\ldots) = a_6 a_5 E - a_7 A, \\ \Theta_5(S_a,\ldots) = (1-a_6)a_5 E - (a_8 + a_9 + a_{10} + a_{11})I, \\ \Theta_6(S_a,\ldots) = a_9 I + a_{12} H_s - (a_3 + a_{14})H_m, \\ \Theta_7(S_a,\ldots) = a_{10} I + a_{14} H_m - (a_{15} + a_{12} + a_{16})H_s, \\ \Theta_8(S_a,\ldots) = a_7 A + a_8 I + a_{13} H_m + a_{15} H_s, \\ \Theta_9(S_a,\ldots) = a_{11} I + a_{16} H_s. \end{cases} \tag{11}$$

With the help of (11), we can write the constructed system as

$$\begin{aligned} {}_0^{\mathrm{ABC}}D_t^{\tau_1} z(t) &= \Theta(t, z(t)), \quad \text{where } t \in [0,T] \\ &\qquad \text{and } 0 < \tau_1 \le 1, \\ z(0) &= z_0. \end{aligned} \tag{12}$$

By making use of Theorem 1, Eq. (12) gives

$$z(t) = z_0(t) + [\Theta(t, z(t)) - \Theta_0(t)]\frac{(1-\tau_1)}{Z(\tau_1)} + \frac{\tau_1}{Z(\tau_1)\Gamma(\tau_1)} \int_0^t \frac{\Theta(\rho, z(\rho))}{(t-\rho)^{1-\tau_1}} d\rho, \tag{13}$$

where

$$z(t) = \begin{cases} S_a(t), \\ S_u(t), \\ E(t), \\ A(t), \\ I(t), \\ H_m(t), \\ H_s(t), \\ R(t), \\ D(t), \end{cases} \qquad z_0(t) = \begin{cases} S_a(0), \\ S_u(0), \\ E(0), \\ A(0), \\ I(0), \\ H_m(0), \\ H_s(0), \\ R(0), \\ D(0) \end{cases} \tag{14}$$

and

$$\Theta(t, z(t)) = \begin{cases} \Theta_1(S_a,\ldots), \\ \Theta_2(S_a,\ldots), \\ \Theta_3(S_a,\ldots), \\ \Theta_4(S_a,\ldots), \\ \Theta_5(S_a,\ldots), \\ \Theta_6(S_a,\ldots), \\ \Theta_7(S_a,\ldots), \\ \Theta_8(S_a,\ldots), \\ \Theta_9(S_a,\ldots), \end{cases}$$

Fractals 2023.31. Downloaded from www.worldscientific.com
by CANKAYA UNIVERSITY on 06/04/24. Re-use and distribution is strictly not permitted, except for Open Access articles.

$$\Theta_0(t) = \begin{cases} \Theta_1(S_{a,0}, S_{u,0}, E_0, A_0 I_0, H_{m,0}, \\ \quad H_{s,0}, R_0, D_0), \\ \Theta_2(S_{a,0}, S_{u,0}, E_0, A_0 I_0, H_{m,0}, \\ \quad H_{s,0}, R_0, D_0), \\ \Theta_3(S_{a,0}, S_{u,0}, E_0, A_0 I_0, H_{m,0}, \\ \quad H_{s,0}, R_0, D_0), \\ \Theta_4(S_{a,0}, S_{u,0}, E_0, A_0 I_0, H_{m,0}, \\ \quad H_{s,0}, R_0, D_0), \\ \Theta_5(S_{a,0}, S_{u,0}, E_0, A_0 I_0, H_{m,0}, \\ \quad H_{s,0}, R_0, D_0), \\ \Theta_6(S_{a,0}, S_{u,0}, E_0, A_0 I_0, H_{m,0}, \\ \quad H_{s,0}, R_0, D_0), \\ \Theta_7(S_{a,0}, S_{u,0}, E_0, A_0 I_0, H_{m,0}, \\ \quad H_{s,0}, R_0, D_0), \\ \Theta_8(S_{a,0}, S_{u,0}, E_0, A_0 I_0, \\ \quad H_{m,0}, H_{s,0}, R_0, D_0), \\ \Theta_9(S_{a,0}, S_{u,0}, E_0, A_0 I_0, H_{m,0}, \\ \quad H_{s,0}, R_0, D_0). \end{cases} \tag{15}$$

Using (13)–(15), define two Φ_1 and Φ_2 using (13)

$$\begin{aligned} \Phi_1 z &= z_0(t) + [\Theta(t, z(t)) - \Theta_0(t)]\frac{(1-\tau_1)}{Z(\tau_1)}, \\ \Phi_2 z &= \frac{\tau_1}{Z(\tau_1)\Gamma(\tau_1)} \int_0^t \frac{\Theta(\rho, z(\rho))}{(t-\rho)^{1-\tau_1}} d\rho. \end{aligned} \tag{16}$$

We assume the following to be true for the creation of Growth constraints, Lipschitzian constraints, and existence with uniqueness.

(l1) $\exists$ constants η_1 and η_2, such that

$$|\Theta(t, z(t))| \leq \eta_1 |z(t)| + \eta_2.$$

(l2) $\exists$ a constant K_1, such that $K_1 > 0$, for every $z, z_1 \in \mathbb{X}$ such that

$$|\Theta(t, z(t)) - \Theta(t, z_1(t))| \leq K_1 \|z - z_1\|.$$

Theorem 3. *If* (l1) *and* (l2) *hold, then it assures that* (l1) *must have one solution at least. This implies* (2) *possesses at least a solution only if*

$$\frac{(1-\tau_1)K_1}{Z(\tau)} < 1. \tag{17}$$

Proof. To get the desired result, that is, Φ_1 is contraction, we take $u_1 \in \mathbb{G}$, where $\mathbb{G} = \{z \in Z^* : \|z\| \leq r^*, r^* > 0\}$ is a set which is closed and convex. Taking Φ_1 from (16), we get

$$\begin{aligned} \|\Phi_1 z - \Phi_1 z_1\| &= \frac{\tau_1}{Z(\tau_1)\Gamma(\tau_1)} \max_{t\in[0,T]} \\ &\quad \times |\Theta(t, z(t)) - \Theta(t, z_1(t))| \\ &\leq \frac{(1-\tau_1)\tau_1}{Z(\tau_1)} \|z - z_1\|. \end{aligned} \tag{18}$$

Therefore, we can claim that Φ_1 is a contraction.

Now, we have to prove that it is relative compactness of Φ_2, for this we need to prove boundedness and continuity of Φ_2. To get the desired results we proceed as follows.

Now, since Θ is continuous so therefore the continuity of Φ_2 is ensured, new for $z \in \mathbb{G}$ as well, we have

$$\begin{aligned} |\Phi_2 z| &= \max_{t\in[0,T]} \frac{\tau_1}{Z(\tau_1)\Gamma(\tau_1)} \left\| \int_0^t \frac{\Theta(\rho, z(\rho))}{(t-\rho)^{1-\tau_1}} d\rho \right\| \\ &\leq \frac{\tau_1}{Z(\tau_1)\Gamma(\tau_1)} \int_0^T \frac{|\Theta(\rho, z(\rho))|}{(t-\rho)^{1-\tau_1}} d\rho \\ &\leq \frac{T^{\tau_1}}{Z(\tau_1)\Gamma(\tau_1)} [\mu_1 r^* + \mu_2]. \end{aligned} \tag{19}$$

Therefore, we claim from (19) that Φ_2 is bounded, for equicontinuity, let $t_1 > t_2 \in [0, T]$, as

$$\begin{aligned} |\Phi_2 z(t_1) - \Phi_2 z(t_2)| &= \frac{\tau_1}{Z(\tau_1)\Gamma(\tau_1)} \left| \int_0^{t_1} \frac{\Theta(\rho, z(\rho))}{(t_1-\rho)^{1-\tau_1}} \right. \\ &\quad \left. \times d\rho - \int_0^{t_2} \frac{\Theta(\rho, z(\rho))}{(t_2-\rho)^{1-\tau_1}} d\rho \right| \\ &\leq \frac{t_1^{\tau_1} - t_2^{\tau_1}}{Z(\tau_1)\Gamma(\tau_1)} [\mu_1 r^* + \mu_2] \end{aligned} \tag{20}$$

whenever $t_1 \to t_2$, the right-hand side of (20) moves to zero, since Φ_2 is continuous and so

$$|\Phi_2 z(t_1) - \Phi_2 z(t_2)| \to 0, \quad \text{as } t_1 \to t_2.$$

It shows that Φ_2 is guaranteed for the boundedness and continuity. It also implies that Φ_2 is uniformly continuous and bounded. Moreover, the Arzelà–Ascoli theorem reveals the relative compactness and thus complete continuity of Φ_2. According to Theorem 3, it can be claimed that Eq. (13) must have at least one solution. Based on the findings in (l2), it can be said that (l1) must have a unique solution thereby the model in (2) will have a unique solution if the inequality given below is satisfied:

$$\frac{(1-\tau_1)K_1}{Z(\tau_1)} + \frac{T^{\tau_1} K_1}{Z(\tau_1)\Gamma(\tau_1)} < 1. \qquad \square$$

Fractals 2023.31. Downloaded from www.worldscientific.com
by CANKAYA UNIVERSITY on 06/04/24. Re-use and distribution is strictly not permitted, except for Open Access articles.

Proof. Let $\mathbb{M}$ be an operator defined as $\mathbb{M} : W \to W^*$ by

$$\mathbb{M}z(t) = z_0(t) + \frac{1-\tau_1}{Z(\tau_1)}[\Theta(t, z(t)) - \Theta_0(t)] + \frac{\tau_1}{Z(\tau_1)\Gamma(\tau_1)} \int_0^t \frac{\Theta(\rho, z(\rho))}{(t-\rho)^{1-\tau_1}} d\rho. \quad (21)$$

Let $z_1, z_2 \in W^*$, then

$$\begin{aligned} &\|\mathbb{M}z_1(t) - \mathbb{M}z_2(t)\| \\ &\quad \le \frac{1-\tau_1}{Z(\tau_1)} \max_{t\in[0,T]} |\Theta(t, z_1(t)) - \Theta(t, z_2)| \\ &\qquad + \frac{\tau_1}{Z(\tau_1)\Gamma(\tau_1)} \max_{t\in[0,T]} \left| \int_0^t \frac{\Theta(\rho, z_1(\rho))}{(t-\rho)^{1-\tau_1}} d\rho \right. \\ &\qquad \left. - \int_0^t \frac{\Theta(\rho, z_2(\rho))}{(t-\rho)^{1-\tau_1}} d\rho \right| \\ &\quad \le \left[\frac{(1-\tau_1)K_1}{Z(\tau)} + \frac{\tau_1 T^{\tau_1} K_1}{Z(\tau)\Gamma(\tau_1)} \right] \|z_1 - z_2\| \\ &\quad \le \Theta \|z_1 - z_2\|, \end{aligned} \quad (22)$$

where

$$\Theta = \frac{(1-\tau_1)K_1}{Z(\tau_1)} + \frac{T^{\tau_1} K_1}{Z(\tau_1)\Gamma(\tau_1)} < 1. \quad (23)$$

From (22), we claim the contraction of $\mathbb{M}$. So, (13) has a unique result. Thus, the system we studied has a unique solution. □

3.2. Stability Analysis of the ABC System

To provide the stability results of the studied model, we make an inconsequential tiny perturbation $\phi \in C[0, T]$, which is dependent on the result only and $\tau_1(0) = 0$. Also

(i) $|\varphi(t)| \le \phi(t)\zeta$, for $\zeta > 0$.
(ii) ${}_0^{\mathrm{ABC}}D_t^{\tau_1} z(t) = \Theta(t, z(t)) + \varphi(t)$, for all $t \in [0, T]$.

Lemma 1. *Solution of the new problem, i.e. perturb problem*

$$\begin{aligned} {}_0^{\mathrm{ABC}}D_t^{\tau_1} z(t) &= \Theta(t, z(t)) + \varphi(t), \\ z(0) &= z_0. \end{aligned} \quad (24)$$

Fulfilling the condition stated below, we have

$$\left| z(t) - \left(z_0(t) + [\Theta(t, z(t)) - \Theta_0(t)] \frac{1-\tau_1}{Z(\tau_1)} + \frac{\tau_1}{Z(\tau_1)\Gamma(\tau_1)} \int_0^t \frac{\Theta(\rho, z(\rho))}{(t-\rho)^{1-\tau_1}} d\rho \right) \right| < M, \quad (25)$$

where

$$M = \frac{(1-\tau_1)\Gamma(\tau_1) + T^{\tau_1}}{Z(\tau_1)\Gamma(\tau_1)}.$$

Proof. The proof is obvious. □

Theorem 4. *From* (l2) *and* (25), *the solution of* (13) *is Ulam–Hyers* (*UH*) *stable and hence the analytical proofs of our proposed system are UH stable if* $\Psi < 1$.

Proof. Let $z_2 \in \mathbb{Z}^*$ represent the first solution and $z_1 \in \mathbb{Z}^*$ represent another solution of (13), then

$$\begin{aligned} &|z_1(t) - z_2(t)| \\ &\quad = \left| z_1(t) - \left(z_{10}(t) + \frac{1-\tau_1}{Z(\tau_1)}[\Theta(t, z_2(t)) - \Theta_0(t)] \right. \right. \\ &\qquad \left. \left. + \frac{\tau_1}{Z(\tau_1)\Gamma(\tau_1)} \int_0^t \frac{\Theta(\rho, z_2(\rho))}{(t-\rho)^{1-\tau_1}} d\rho \right) \right| \\ &\quad \le \left| z_1(t) - \left(z_{10}(t) + \frac{1-\tau_1}{Z(\tau_1)}[\Theta(t, z_1(t)) - \Theta_0(t)] \right. \right. \\ &\qquad \left. \left. + \frac{\tau_1}{Z(\tau_1)\Gamma(\tau_1)} \int_0^t \frac{\Theta(\rho, z_1(\rho))}{(t-\rho)^{1-\tau_1}} d\rho \right) \right| \\ &\qquad + \left| \left(z_{10}(t) + \frac{1-\tau_1}{Z(\tau_1)}[\Theta(t, z_1(t)) - \Theta_0(t)] \right. \right. \\ &\qquad \left. \left. + \frac{\tau_1}{Z(\tau_1)\Gamma(\tau_1)} \int_0^t \frac{\Theta(\rho, z_1(\rho))}{(t-\rho)^{1-\tau_1}} d\rho \right) \right. \\ &\qquad \left. - \left(z_{10}(t) + \frac{1-\tau_1}{Z(\tau_1)}[\Theta(t, z_2(t)) - \Theta_0(t)] \right. \right. \\ &\qquad \left. \left. + \frac{\tau_1}{Z(\tau_1)\Gamma(\tau_1)} \int_0^t \frac{\Theta(\rho, z_2(\rho))}{(t-\rho)^{1-\tau_1}} d\rho \right) \right| \\ &\quad \le \zeta M + \frac{(1-\tau_1)K_1}{Z(\tau_1)} \|z_1 - z_2\| \\ &\qquad + \frac{T^{\tau_1} K_1}{Z(\tau_1)\Gamma(\tau_1)} \|z_1 - z_2\| \\ &\quad \le \zeta M + \Theta \|z_1 - z_2\|. \end{aligned} \quad (26)$$

From (26), we can write

$$\|z_1 - z_2\| = \frac{\zeta M}{1 - \Theta}. \quad (27)$$

□

From (27), it has been claimed that the solution of (13) is UH stable and therefore generalized UH (gUH) stable by making use of $\Theta_z(\zeta) = M\zeta$, $\Theta_z(0) = 0$, which clears the proposed problem has UH and gUH stable solution.

Fractals 2023.31. Downloaded from www.worldscientific.com by CANKAYA UNIVERSITY on 06/04/24. Re-use and distribution is strictly not permitted, except for Open Access articles.

Now, let us suppose

(i) $|\varphi(t)| \leq \phi(t)\zeta$, for $\zeta > 0$.
(ii) ${}_0^{\mathrm{ABC}}D_t^{\tau_1} z(t) = \Theta(t, z(t)) + \varphi(t)$, for all $t \in [0, T]$.

Lemma 2. *From* (24), *the inequality given below holds*

$$\left| z(t) - \left(z_0(t) + [\Theta(t, z(t)) - \Theta_0(t)] \frac{1-\tau_1}{Z(\tau_1)} + \frac{\tau_1}{Z(\tau_1)\Gamma(\tau_1)} \int_0^t \frac{\Theta(\rho, z(\rho))}{(t-\rho)^{1-\tau_1}} d\rho \right) \right| \leq \phi(t)\zeta M. \tag{28}$$

Proof. The proof is straightforward. □

Theorem 5. *From lemma* (28), *we declare that the considered problem has the stability of Ulam–Hyers–Rassias (UHR) type stable and therefore of gUHR.*

Proof. Let $z_1, z_2 \in Z^*$, where z_1 and z_2 represent the two solutions of (13), then

$$\begin{aligned}
&|z_1(t) - z_2(t)| \\
&= \left| z_1(t) - \left(z_{10}(t) + \frac{1-\tau_1}{Z(\tau_1)} [\Theta(t, z_2(t)) - \Theta_0(t)] + \frac{\tau_1}{Z(\tau_1)\Gamma(\tau_1)} \int_0^t \frac{\Theta(\rho, z_2(\rho))}{(t-\rho)^{1-\tau_1}} d\rho \right) \right| \\
&\leq \left| z_1(t) - \left(z_{10}(t) + \frac{1-\tau_1}{Z(\tau_1)} [\Theta(t, z_1(t)) - \Theta_0(t)] + \frac{\tau_1}{Z(\tau_1)\Gamma(\tau_1)} \int_0^t \frac{\Theta(\rho, z_1(\rho))}{(t-\rho)^{1-\tau_1}} d\rho \right) \right| \\
&\quad + \left| \left(z_{10}(t) + \frac{1-\tau_1}{Z(\tau_1)} [\Theta(t, z_1(t)) - \Theta_0(t)] + \frac{\tau_1}{Z(\tau_1)\Gamma(\tau_1)} \int_0^t \frac{\Theta(\rho, z_1(\rho))}{(t-\rho)^{1-\tau_1}} d\rho \right) \right. \\
&\quad \left. - \left(z_{10}(t) + \frac{1-\tau_1}{Z(\tau_1)} [\Theta(t, z_2(t)) - \Theta_0(t)] + \frac{\tau_1}{Z(\tau_1)\Gamma(\tau_1)} \int_0^t \frac{\Theta(\rho, z_2(\rho))}{(t-\rho)^{1-\tau_1}} d\rho \right) \right| \\
&\leq \phi(t)\zeta M + \frac{(1-\tau_1)K_1}{Z(\tau_1)} \|z_1 - z_2\| + \frac{T^{\tau_1} K_1}{Z(\tau_1)\Gamma(\tau_1)} \|z_1 - z_2\| \\
&\leq \phi(t)\zeta M + \Theta \|z_1 - z_2\|.
\end{aligned} \tag{29}$$

From (29), we can write

$$\|z_1 - z_2\| = \frac{\phi(t)\zeta M}{1 - \Theta}. \tag{30}$$

Therefore, we say that the results of (13) are UHR stable and consequently gUHR stable. □

3.3. Estimation of Biological Parameters

When a new epidemiological model is designed, its validation is one of the crucial tasks to have some reliability of the proposed model. The task is crucial because, in most cases, the accurately collected data set is not available, and even if it is found, it has some measurement errors and uncertainties. This leads to having misleading values of the assumed biological parameters introduced in the proposed model based on certain assumptions. In this research study, we have obtained real observations for the COVID-19 cumulative cases via a reliable source from the Nigeria Centre for Disease Control (NCDC).[30]

As it comes to estimate the unknown parameters, several authors use a technique known as the nonlinear least-squares curve fitting technique. MATLAB software's help is sought in this regard while using its built-in routine with the name of "*fminsearch*" available from the `MATLAB` Optimization Toolbox. According to this approach, when a proposed theoretical model $t \mapsto \Omega(t, s_1, s_2, \ldots, s_n)$ is obtained that completely depends on some unknown parameters such as $s_1, s_2, \ldots, s_n$ and a sequence of real observations $(t_0, y_0), \ldots, (t_j, y_j)$ is also available then the objective is to achieve values of the parameters for which the computed residual error

$$\text{Residual} := \sqrt{\sum_{i=0}^{n} (\Omega(t, s_1, s_2, \ldots, s_n) - y_i)^2} \tag{31}$$

attains a minimum. There are both fixed and unknown biological parameters associated with the proposed model. The fixed parameters are obtained from the existing literature whereas unknown parameters are obtained (fitted) with the technique mentioned earlier. As can be seen in Table 1, the parameters' values are listed. The initial conditions for the model's state variables are estimated as $S_a(0) = 130000000$, $S_u(0) = 76000000$, $E(0) = 22$, $A(0) = 10$, $I(0) = 111$, $H_m(0) = 5$, $H_s(0) = 0$, $R(0) = 0$, and $D(0) = 0$. The choice of initial conditions, fixed and fitted biological parameters

Fractals 2023.31. Downloaded from www.worldscientific.com
by CANKAYA UNIVERSITY on 06/04/24. Re-use and distribution is strictly not permitted, except for Open Access articles.

Table 1 Baseline Values of the Parameters Used in the Model (1).

Fitted Parameter	Value (Range)	Units/Remarks	Sources
a_4	0.01738 (0.01–0.5)	day^{-1}	Fitted
a_1	0.30659 (0.01–0.95)	day^{-1}	Fitted
a_2	0.84801 (0.599–1.68)	day^{-1}	Fitted
a_3	0.06750 (0.04–0.6)	day^{-1}	Fitted
a_5	0.87959 (0.05–0.95)	day^{-1}	Fitted
a_6	0.01632 (0–1)	day^{-1}	Fitted
a_7	0.03671 (1/28–1/3)	day^{-1}	Fitted
a_8	0.00917 (1/1000–1/3)	day^{-1}	Fitted
a_{12}	0.16906 (0.001–0.5)	day^{-1}	Fitted
Parameters from the literature			
a_{13}	0.11624 (0–1)	day^{-1}	Refs. 32 and 33
a_{15}	0.155 (0–1)	day^{-1}	Refs. 32 and 33
a_{11}	0.015 (0.01–0.05)	day^{-1}	Ref. 32
a_{16}	0.025 (0.01–0.05)	day^{-1}	Ref. 32
a_9	0.1259 (0.09–0.51)	day^{-1}	Refs. 32 and 33
a_{10}	0.13266 (0.001–0.5)	day^{-1}	Ref. 33
a_{14}	0.0341 (0.001–0.5)	day^{-1}	Ref. 32

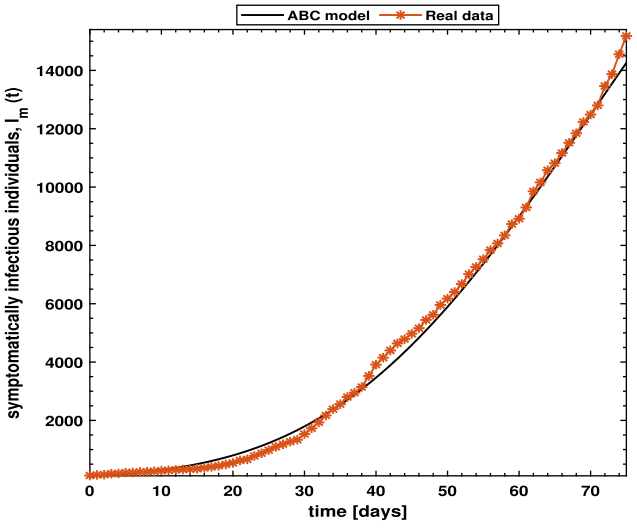

Fig. 1 The cumulative cases on daily basis for COVID-19 pandemic in Nigeria from March 29 to June 12, 2020 with the best fitted curve from simulations of the ABC model.

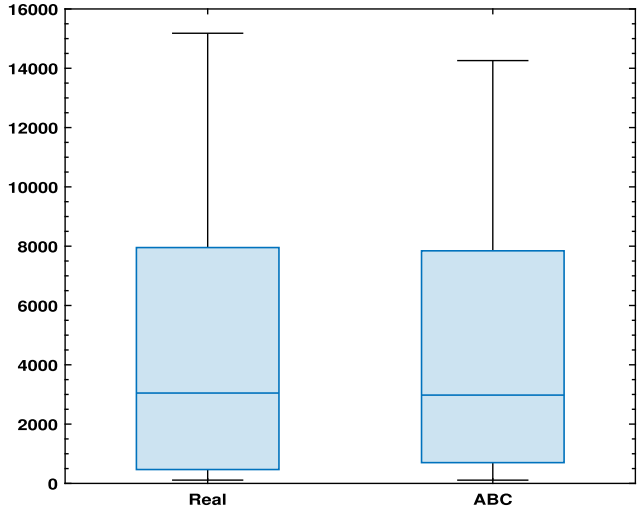

Fig. 2 The box and whisker plot for comparison of the statistical measures between real observations of COVID-19 and the predicted observations under the ABC model.

yielded the average absolute relative error of magnitude $1.2764e-01$ which is reasonably small enough and also smaller than the residual error obtained via classical version of the proposed model.

Moreover, real observations for the COVID-19 Nigerian cases and the fitted curve from the ABC version of the model are shown in Fig. 1. It is observed that the infected class of the ABC model perfectly fits the real observations. The same is also confirmed via box and whisker plot as shown in Fig. 2. The residuals can be obtained from (31). Finally, the basic reproductive number ($\mathcal{R}_0$) is estimated as $= 1.6737$ (95%CI : $5.8725e-02$ — 2.8728) using the parameters presented in Table 1 whereas the summary statistics obtained with the real and predicted (ABC) observations are calculated in Table 2. This result is largely consistent with the previous estimate on the basic reproduction number ($\mathcal{R}_0$) in Africa.[31] Subsequently, the $\mathcal{R}_0$ value will increase (i.e. $\mathcal{R}_0 = 2.98$) if all the awareness-related parameters are discarded, indicating the positive impacts of awareness programs

Table 2 Summary Statistics for the Actual COVID-19 Observations, and the Predicted Observations Via ABC Operator.

Data	Min.	1st Qu.	Median	Mean	3rd Qu.	Max.
Real	$1.1100e+02$	$4.6750e+02$	$3.0475e+03$	$4.6235e+03$	$7.9535e+03$	$1.5181e+04$
ABC	$1.0982e+02$	$7.0045e+02$	$2.9783e+03$	$4.5595e+03$	$7.8439e+03$	$1.4259e+04$

on curtailing the distribution of the COVID-19 pandemic in Nigeria and beyond. One of the most important points to be noted is that the fractional-order parameter τ under the ABC operator is also optimized whose optimal value is obtained to be $9.9810e-01$.

4. NUMERICAL SIMULATIONS

In this section, we present the predictor–corrector approach, an effective approximation scheme for the numerical solution of the fractional differential equation (2). It should be noted that this approach has already been examined for fractional differential equations in Ref. 34. To develop this method for Eq. (2) in the sense of ABC fractional derivative. Consider a uniform mesh on $[0.T]$ and label the nodes $0, 1, 2, \ldots, Nh$, where Nh is an arbitrary positive integer and $h = \frac{T-0}{Nh}$ is the time step size. Now to find the approximate solution of the proposed model we apply Theorem 1 to each of S_a, S_u, E, A, I, H_m, H_s, R, D of the system (2), we get the results as follows:

$$\begin{cases} g_1(t) = -\dfrac{a_1 a_2 S_a(t)}{N}(a_3 A(t) + I(t)) + a_4 S_u(t), \\ g_2(t) = -\dfrac{a_2 S_u(t)}{N}(a_3 A(t) + I(t)) - a_4 S_u(t), \\ g_3(t) = \dfrac{a_2}{N}(a_3 A(t) + I(t))(a_1 S_a(t) \\ \qquad + S_u(t)) - a_5 E(t), \\ g_4(t) = a_6 a_5 E(t) - a_7 A(t), \\ g_5(t) = (1 - a_6) a_5 E(t) - (a_8 + a_9 + a_{10} \\ \qquad + a_{11}) I(t), \\ g_6(t) = a_9 I(t) + a_{12} H_s(t) - (a_3 \\ \qquad + a_{14}) H_m(t), \\ g_7(t) = a_{10} I(t) + a_{14} H_m(t) - (a_{15} + a_{12} \\ \qquad + a_{16}) H_s(t), \\ g_8(t) = a_7 A(t) + a_8 I(t) + a_{13} H_m(t) + a_{15} H_s(t), \\ g_9(t) = a_{11} I(t) + a_{16} H_s(t), \end{cases} \tag{32}$$

$$\begin{cases} S_a(t_{i+1}) = S_{a,0} + \dfrac{1-\tau_1}{Z(\tau_1)} g_1(t_{i+1}^Q) \\ \qquad + \dfrac{\tau_1 h^{\tau_1}}{Z(\tau_1)\Gamma(\tau_1)} \left[\sum_{j=0}^{i} a_{i+1,j} g_1(t_j) \right. \\ \qquad \left. + a_{i+1,j+1} g_1(t_{i+1}^Q) \right], \\ S_u(t_{i+1}) = S_{u,0} + \dfrac{1-\tau_1}{Z(\tau_1)} g_2(t_{i+1}^Q) \\ \qquad + \dfrac{\tau_1 h^{\tau_1}}{Z(\tau_1)\Gamma(\tau_1)} \left[\sum_{j=0}^{i} a_{i+1,j} g_2(t_j) \right. \\ \qquad \left. + a_{i+1,j+1} g_2(t_{i+1}^Q) \right], \\ E(t_{i+1}) = E_0 + \dfrac{1-\tau_1}{Z(\tau_1)} g_3(t_{i+1}^Q) \\ \qquad + \dfrac{\tau_1 h^{\tau_1}}{Z(\tau_1)\Gamma(\tau_1)} \left[\sum_{j=0}^{i} a_{i+1,j} g_3(t_j) \right. \\ \qquad \left. + a_{i+1,j+1} g_3(t_{i+1}^Q) \right], \\ A(t_{i+1}) = A_0 + \dfrac{1-\tau_1}{Z(\tau_1)} g_4(t_{i+1}^Q) \\ \qquad + \dfrac{\tau_1 h^{\tau_1}}{Z(\tau_1)\Gamma(\tau_1)} \left[\sum_{j=0}^{i} a_{i+1,j} g_4(t_j) \right. \\ \qquad \left. + a_{i+1,j+1} g_4(t_{i+1}^Q) \right], \\ I(t_{i+1}) = I_0 + \dfrac{1-\tau_1}{Z(\tau_1)} g_5(t_{i+1}^Q) \\ \qquad + \dfrac{\tau_1 h^{\tau_1}}{Z(\tau_1)\Gamma(\tau_1)} \left[\sum_{j=0}^{i} a_{i+1,j} g_5(t_j) \right. \\ \qquad \left. + a_{i+1,j+1} g_5(t_{i+1}^Q) \right], \end{cases}$$

Fractals 2023.31. Downloaded from www.worldscientific.com by CANKAYA UNIVERSITY on 06/04/24. Re-use and distribution is strictly not permitted, except for Open Access articles.

Fractals 2023.31. Downloaded from www.worldscientific.com
by CANKAYA UNIVERSITY on 06/04/24. Re-use and distribution is strictly not permitted, except for Open Access articles.

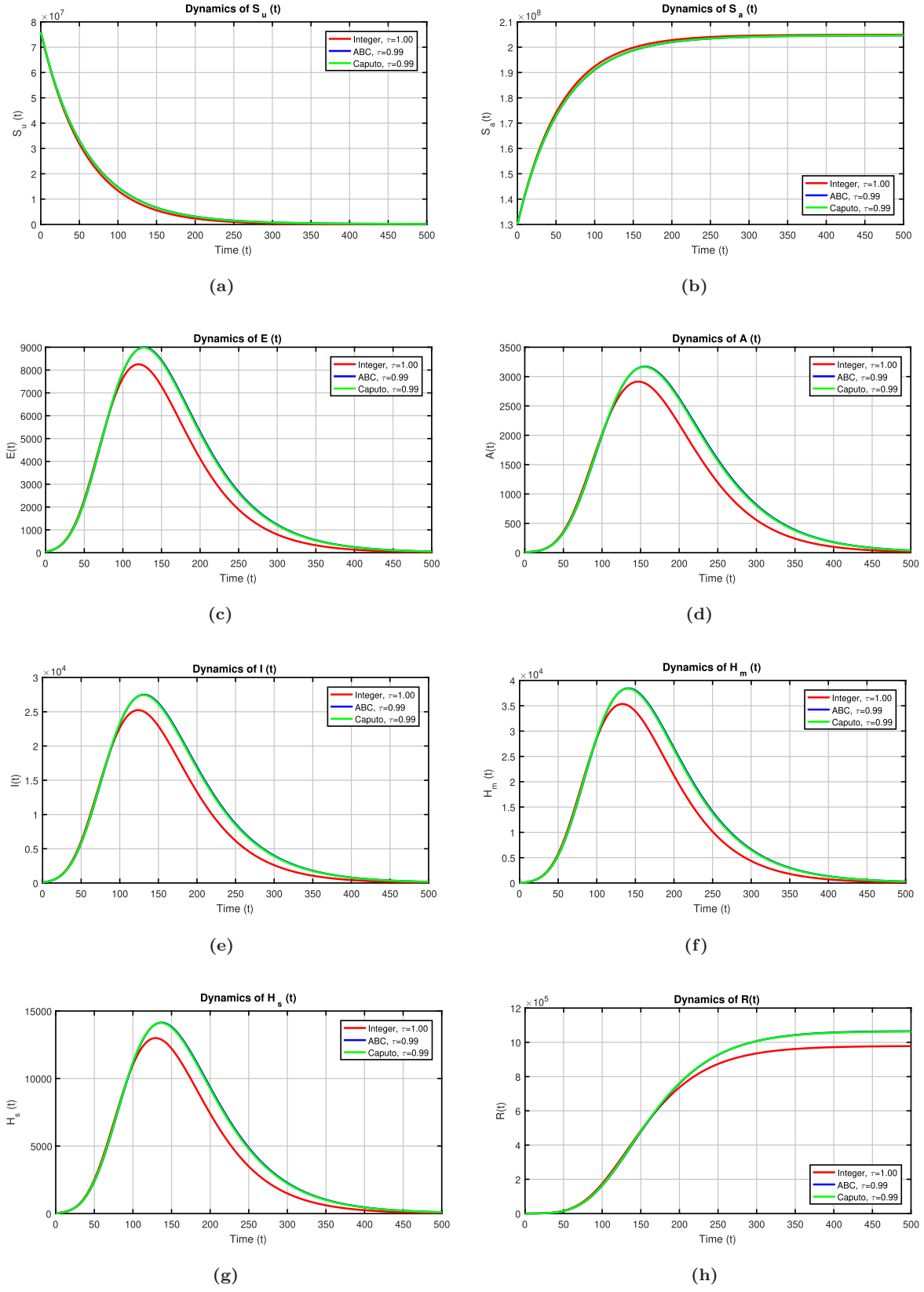

Fig. 3 Time series plots for the simulation of the model (2) showing the dynamical behavior using three techniques with fractional index $\tau_1 = 0.99$ over time interval $[0, 500]$ while using the parameters' values given in Table 1.

Fractals 2023.31. Downloaded from www.worldscientific.com
by CANKAYA UNIVERSITY on 06/04/24. Re-use and distribution is strictly not permitted, except for Open Access articles.

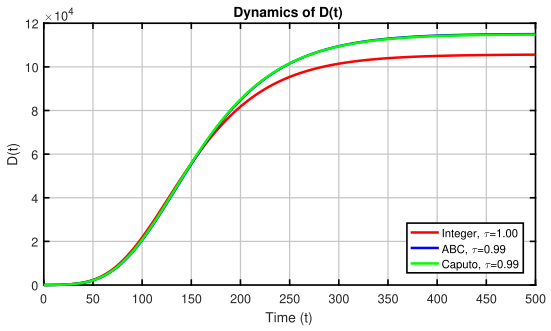

(i)

Fig. 3 (*Continued*)

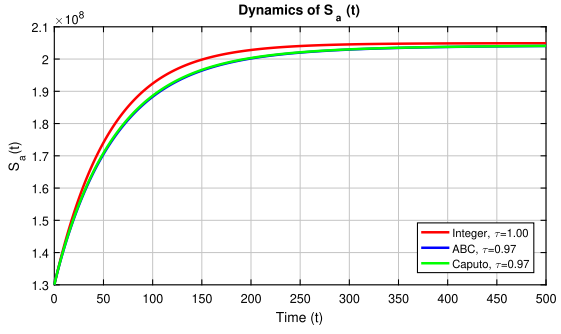

(a)

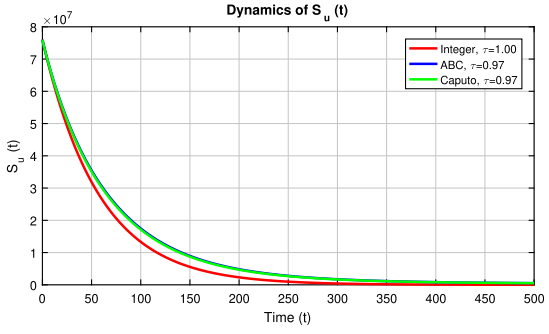

(b)

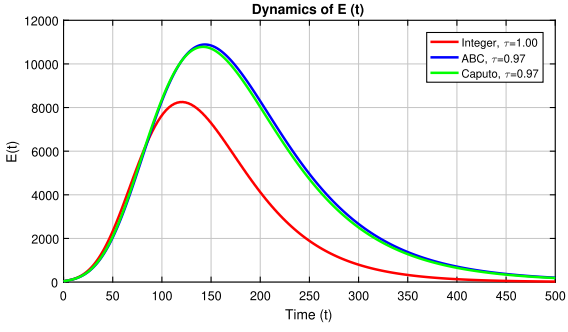

(c)

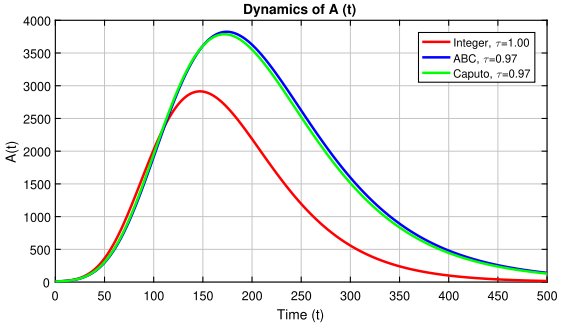

(d)

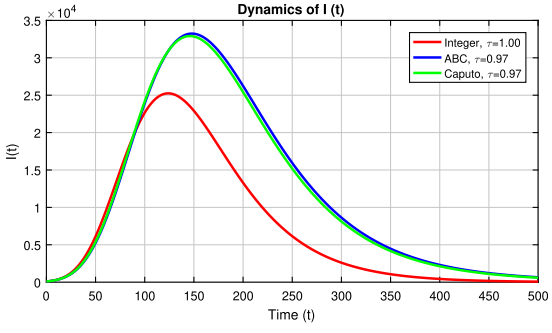

(e)

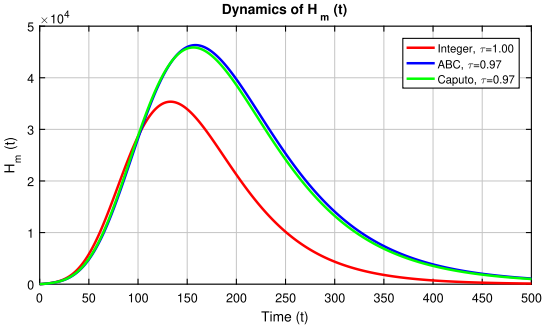

(f)

Fig. 4 Time series plots for the simulation of the model (2) showing the dynamical behavior using three techniques with fractional index $\tau_1 = 0.97$ over time interval $[0, 500]$ while using the parameters' values given in Table 1.

Fractals 2023.31. Downloaded from www.worldscientific.com
by CANKAYA UNIVERSITY on 06/04/24. Re-use and distribution is strictly not permitted, except for Open Access articles.

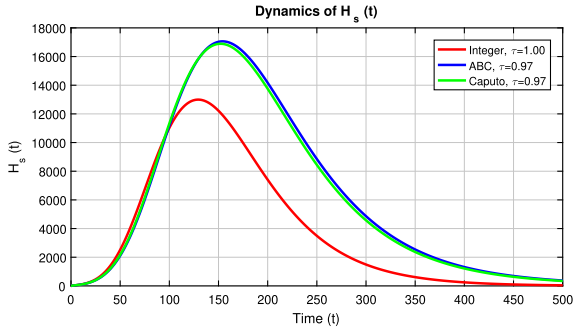

(g)

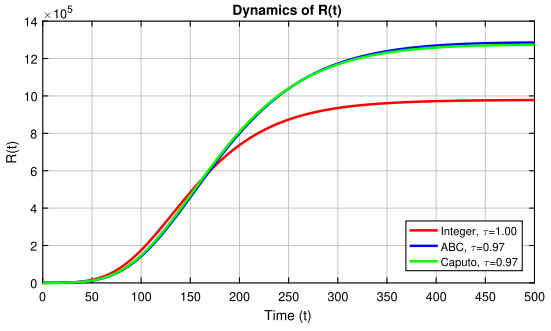

(h)

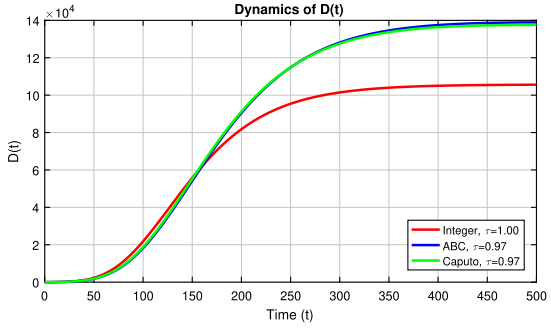

(i)

Fig. 4 (*Continued*)

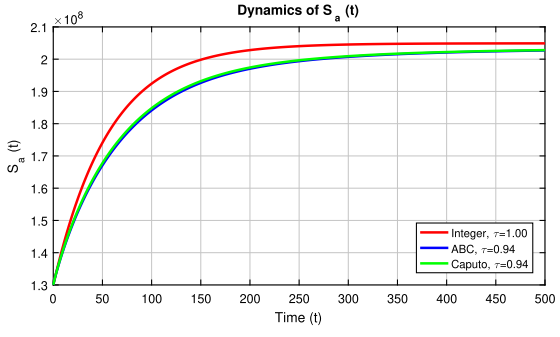

(a)

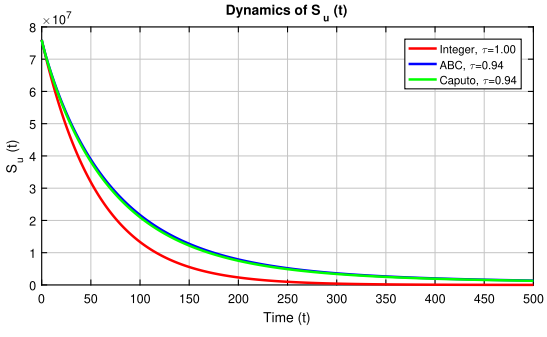

(b)

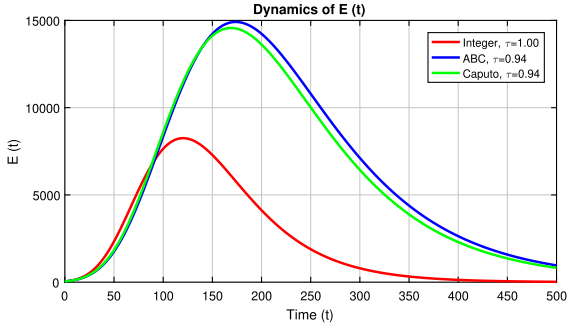

(c)

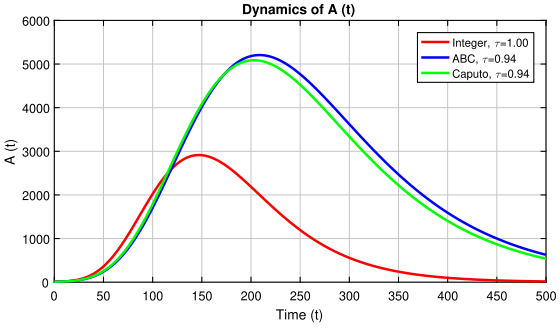

(d)

Fig. 5 Time series plots for the simulation of the model (2) showing the dynamical behavior using three techniques with fractional index $\tau_1 = 0.94$ over time interval $[0, 500]$ while using the parameters' values given in Table 1.

Fractals 2023.31. Downloaded from www.worldscientific.com
by CANKAYA UNIVERSITY on 06/04/24. Re-use and distribution is strictly not permitted, except for Open Access articles.

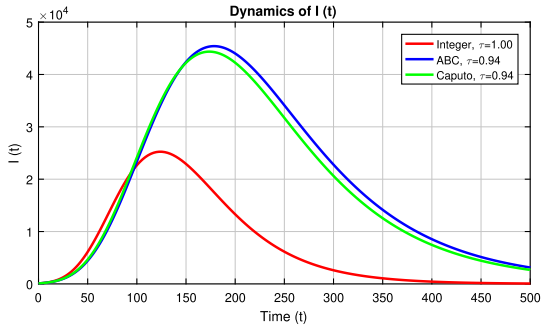

(e)

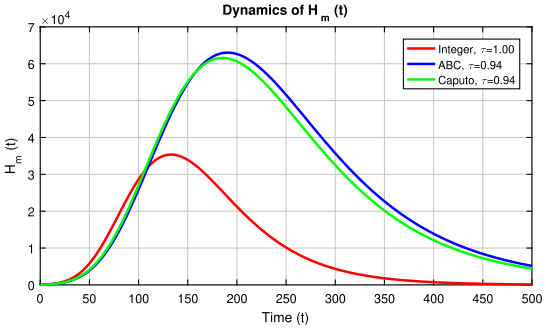

(f)

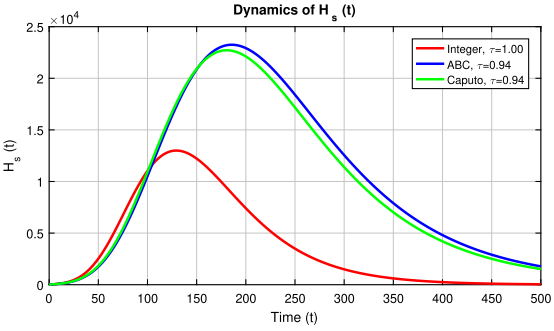

(g)

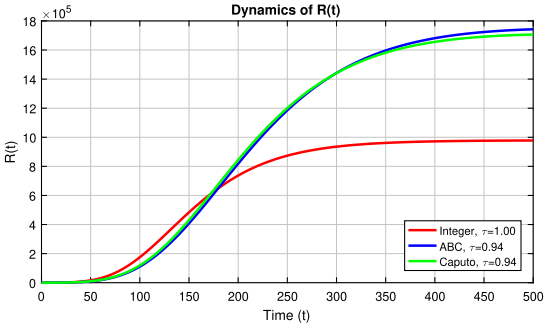

(h)

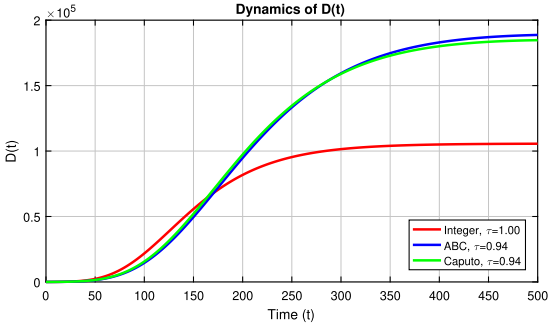

(i)

Fig. 5 (*Continued*)

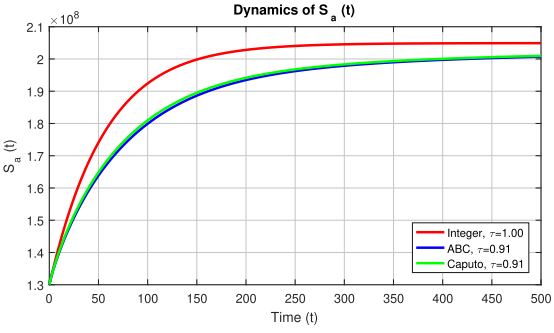

(a)

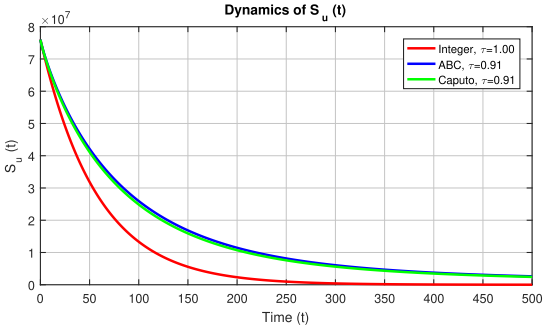

(b)

Fig. 6 Time series plots for the simulation of the model (2) showing the dynamical behavior using three techniques with fractional index $\tau_1 = 0.91$ over time interval $[0, 500]$ while using the parameters' values given in Table 1.

Fractals 2023.31. Downloaded from www.worldscientific.com
by CANKAYA UNIVERSITY on 06/04/24. Re-use and distribution is strictly not permitted, except for Open Access articles.

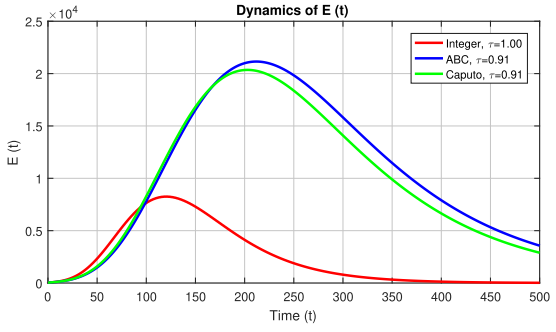

(c)

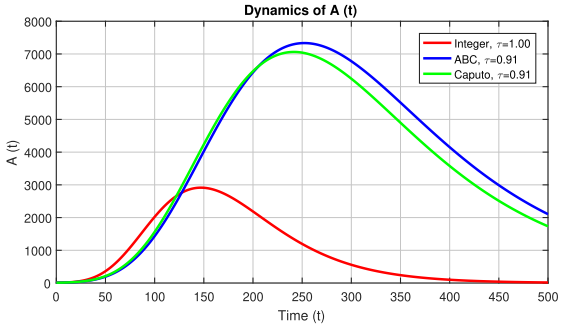

(d)

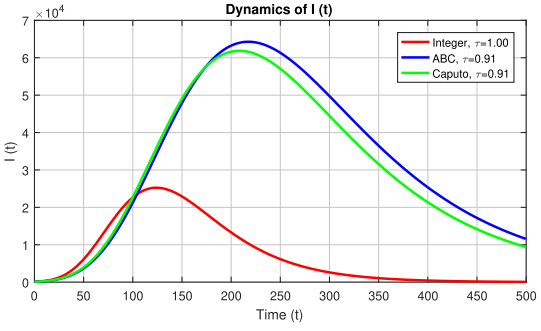

(e)

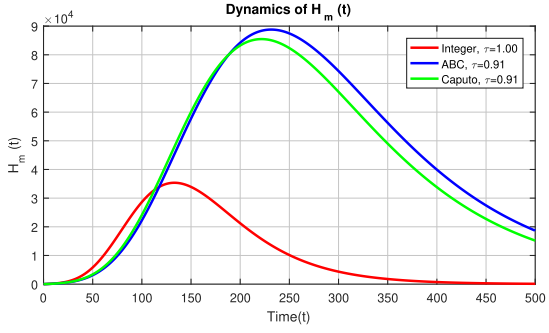

(f)

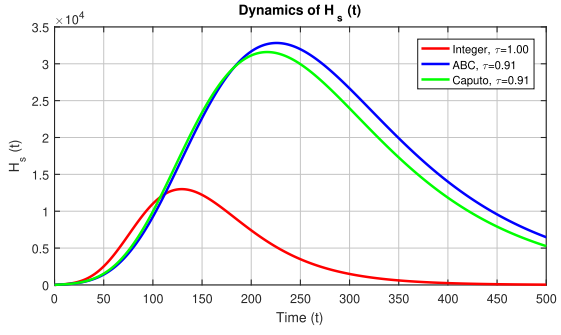

(g)

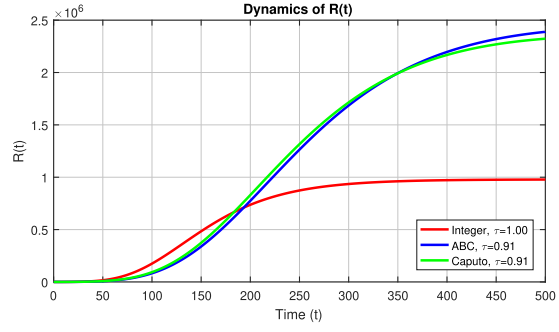

(h)

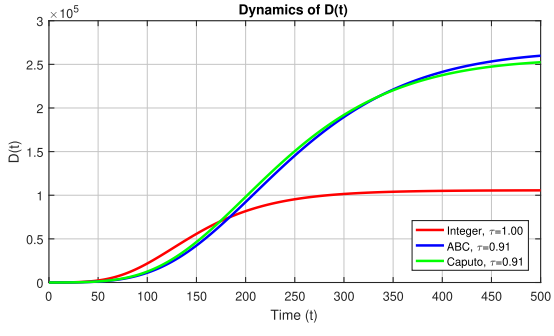

(i)

Fig. 6 (*Continued*)

Fractals 2023.31. Downloaded from www.worldscientific.com
by CANKAYA UNIVERSITY on 06/04/24. Re-use and distribution is strictly not permitted, except for Open Access articles.

$$\begin{cases} H_m(t_{i+1}) = H_{m,0} + \dfrac{1-\tau_1}{Z(\tau_1)} g_6(t^Q_{i+1}) \\ \qquad + \dfrac{\tau_1 h^{\tau_1}}{Z(\tau_1)\Gamma(\tau_1)} \left[\displaystyle\sum_{j=0}^{i} a_{i+1,j} g_6(t_j) \right. \\ \qquad \left. + a_{i+1,j+1} g_6(t^Q_{i+1}) \right], \\ H_s(t_{i+1}) = H_{s,0} + \dfrac{1-\tau_1}{Z(\tau_1)} g_7(t^Q_{i+1}) \\ \qquad + \dfrac{\tau_1 h^{\tau_1}}{Z(\tau_1)\Gamma(\tau_1)} \left[\displaystyle\sum_{j=0}^{i} a_{i+1,j} g_7(t_j) \right. \\ \qquad \left. + a_{i+1,j+1} g_7(t^Q_{i+1}) \right], \\ R(t_{i+1}) = R_0 + \dfrac{1-\tau_1}{Z(\tau_1)} g_8(t^Q_{i+1}) \\ \qquad + \dfrac{\tau_1 h^{\tau_1}}{Z(\tau_1)\Gamma(\tau_1)} \left[\displaystyle\sum_{j=0}^{i} a_{i+1,j} g_8(t_j) \right. \\ \qquad \left. + a_{i+1,j+1} g_8(t^Q_{i+1}) \right], \\ D(t_{i+1}) = D_0 + \dfrac{1-\tau_1}{Z(\tau_1)} g_9(t^Q_{i+1}) \\ \qquad + \dfrac{\tau_1 h^{\tau_1}}{Z(\tau_1)\Gamma(\tau_1)} \left[\displaystyle\sum_{j=0}^{i} a_{i+1,j} g_9(t_j) \right. \\ \qquad \left. + a_{i+1,j+1} g_9(t^Q_{i+1}) \right], \end{cases} \tag{33}$$

and

$$\begin{cases} S_a(t^Q_{i+1}) = S_{a,0} + \dfrac{1-\tau_1}{Z(\tau_1)} g_1(t_i) + \dfrac{h^{\tau_1}}{Z(\tau_1\Gamma(\tau_1))} \\ \qquad \times \displaystyle\sum_{j=0}^{i} b_{i+1,j} g_1(t_j), \\ S_u(t^Q_{i+1}) = S_{u,0} + \dfrac{1-\tau_1}{Z(\tau_1)} g_2(t_i) + \dfrac{h^{\tau_1}}{Z(\tau_1\Gamma(\tau_1))} \\ \qquad \times \displaystyle\sum_{j=0}^{i} b_{i+1,j} g_2(t_j), \\ E(t^Q_{i+1}) = E_0 + \dfrac{1-\tau_1}{Z(\tau_1)} g_3(t_i) + \dfrac{h^{\tau_1}}{Z(\tau_1\Gamma(\tau_1))} \\ \qquad \times \displaystyle\sum_{j=0}^{i} b_{i+1,j} g_3(t_j), \\ A(t^Q_{i+1}) = A_0 + \dfrac{1-\tau_1}{Z(\tau_1)} g_4(t_i) + \dfrac{h^{\tau_1}}{Z(\tau_1\Gamma(\tau_1))} \\ \qquad \times \displaystyle\sum_{j=0}^{i} b_{i+1,j} g_4(t_j), \\ I(t^Q_{i+1}) = I_0 + \dfrac{1-\tau_1}{Z(\tau_1)} g_5(t_i) + \dfrac{h^{\tau_1}}{Z(\tau_1\Gamma(\tau_1))} \\ \qquad \times \displaystyle\sum_{j=0}^{i} b_{i+1,j} g_5(t_j), \\ H_m(t^Q_{i+1}) = H_{m,0} + \dfrac{1-\tau_1}{Z(\tau_1)} g_6(t_i) + \dfrac{h^{\tau_1}}{Z(\tau_1\Gamma(\tau_1))} \\ \qquad \times \displaystyle\sum_{j=0}^{i} b_{i+1,j} g_6(t_j), \\ H_s(t^Q_{i+1}) = H_{s,0} + \dfrac{1-\tau_1}{Z(\tau_1)} g_7(t_i) + \dfrac{h^{\tau_1}}{Z(\tau_1\Gamma(\tau_1))} \\ \qquad \times \displaystyle\sum_{j=0}^{i} b_{i+1,j} g_7(t_j), \\ R(t^Q_{i+1}) = R_0 + \dfrac{1-\tau_1}{Z(\tau_1)} g_8(t_i) + \dfrac{h^{\tau_1}}{Z(\tau_1\Gamma(\tau_1))} \\ \qquad \times \displaystyle\sum_{j=0}^{i} b_{i+1,j} g_8(t_j), \\ D(t^Q_{i+1}) = D_0 + \dfrac{1-\tau_1}{Z(\tau_1)} g_9(t_i) + \dfrac{h^{\tau_1}}{Z(\tau_1\Gamma(\tau_1))} \\ \qquad \times \displaystyle\sum_{j=0}^{i} b_{i+1,j} g_9(t_j), \end{cases} \tag{34}$$

where $a_{i+1,j}$ and $b_{i+1,j}$ are given in (9) and (10).

The influence of awareness programs on the dynamics of COVID-19 is investigated in this section by simulating the awareness-related parameters of the model (2) across the time span $[0, 500]$. The suggested model (1) is simulated using the beginning circumstances and settings supplied in Sec. 3.3 under three scenarios presented below. Also, we are giving the plots for different values

Fractals 2023.31. Downloaded from www.worldscientific.com
by CANKAYA UNIVERSITY on 06/04/24. Re-use and distribution is strictly not permitted, except for Open Access articles.

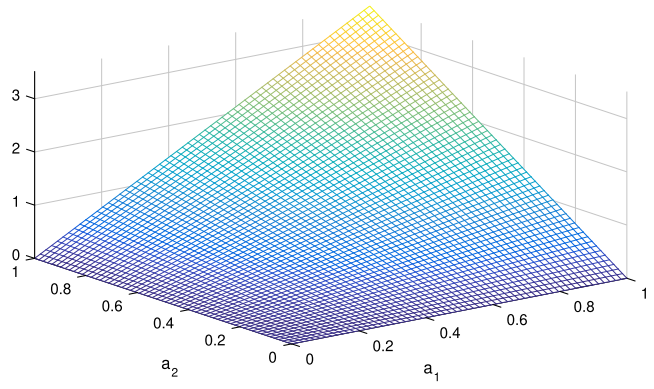

Fig. 7 The plot demonstrates the variation of $\mathcal{R}_0$ against a_1 and a_2.

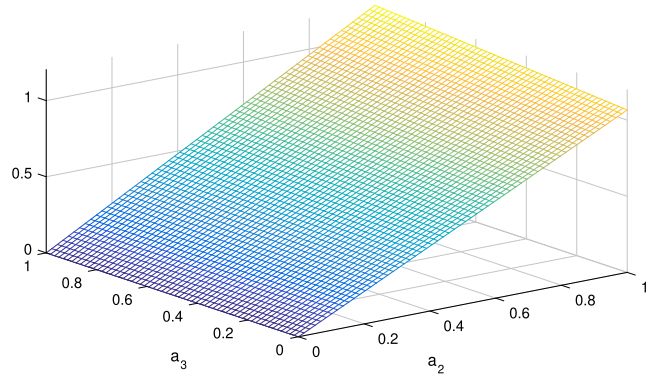

Fig. 8 The plot demonstrates the variation of $\mathcal{R}_0$ against a_2 and a_3.

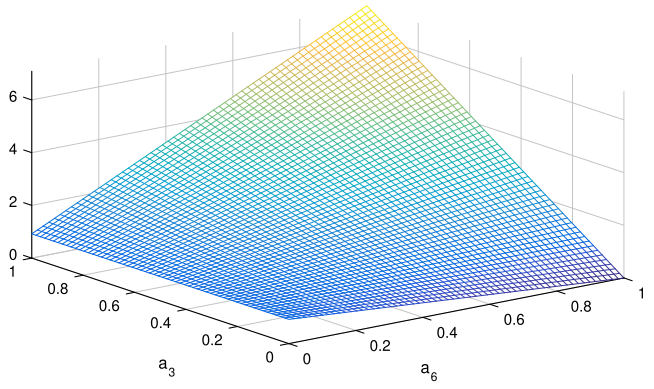

Fig. 9 The plot demonstrates the variation of $\mathcal{R}_0$ against a_6 and a_3.

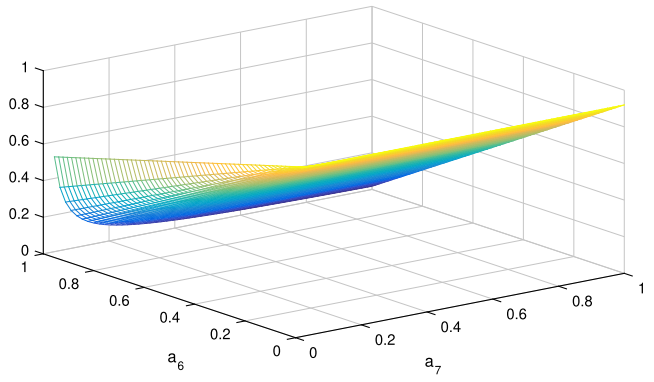

Fig. 10 The plot demonstrates the variation of $\mathcal{R}_0$ against a_7 and a_6.

of fractional order τ_1. The step size during simulations is taken to be $h = 10^{-2}$ where Nh $=$ 500. Additionally, simulations were produced using the Atangana–Baleanu predictor corrector method in MATLAB software, which is running on a 64-bit Windows operating system with an Intel(R) Core(TM) i5-7200U CPU running at 2.50 GHz and 4.0 GB of installed memory (RAM).

5. SENSITIVITY ANALYSIS

Sensitive analysis helps us to see the variation in the variables when changing the parameters occurring in the $\mathcal{R}_0$. It tells us which component of $\mathcal{R}_0$ plays a vital role in the model under observed.

Definition (Ref. 35). The normalized forward sensitivity index of the basic reproduction number $\mathcal{R}_0$ that depends on a parameter μ is given as

$$H_\mu = \frac{\mu}{\mathcal{R}_0}\frac{\partial \mathcal{R}_0}{\partial \mu}. \tag{35}$$

To calculate the sensitivity indices, one of the three techniques, namely (a) linearization method, (b) Latin hypercube sampling method, and (c) direct differentiation method can be used and then the consequences obtained can be solved using any technique. Over here, category (c) is used. The indices help us identify which indices have positive influence and which have negative impact. It also helps in developing strategies to control disease.

The positive influence of the parameters a_1, a_2, and a_3 on the basic reproduction number $\mathcal{R}_0$ is reflected in Table 3 wherein it can be observed that the growth (decay) in the values of these parameters would bring an increase (decrease) in $\mathcal{R}_0$. For example, if 10% of the parameters are increased, there will be a corresponding 10%, 0.08%, and 10% increase in $\mathcal{R}_0$ as depicted by the table. On the other hand, there will be approximately 0.07%, 0.08%, 0.3%, 4.4%, 4.6%, and 0.5% decrease in the value of $\mathcal{R}_0$ if the index for parameters a_6, a_7, a_8, a_9, a_{10}, and a_{11} is increased by 10%.

Table 3 Sensitivity Indices of the Reproduction Number $\mathcal{R}_0$ Against Mentioned Parameters.

Parameters	S. Index	Value	Parameters	S. Index	Value
a_1	H_{a_1}	1.00000000	a_8	H_{a_8}	−0.03216947
a_2	H_{a_2}	1.00000000	a_9	H_{a_9}	−0.44148758
a_3	H_{a_3}	0.00855060	a_{10}	$H_{a_{10}}$	−0.46519256
a_6	H_{a_6}	−0.00789615	a_{11}	$H_{a_{11}}$	−0.05259979
a_7	H_{a_7}	−0.00855060			

Fractals 2023.31. Downloaded from www.worldscientific.com
by CANKAYA UNIVERSITY on 06/04/24. Re-use and distribution is strictly not permitted, except for Open Access articles.

6. CONCLUDING REMARKS

Many epidemiological and clinical aspects remain limited to date since the COVID-19 pandemic is still fresh and evolving. Most reports and studies done thus far have used relatively small samples. When all of these papers and studies are combined, the details of COVID-19 become apparent, allowing policymakers to make better decisions. Using NPIs to fight the SARS-CoV-2 epidemic continues to be an important tactic. A worldwide effort to raise public awareness about the dangers of COVID-19 is essential if we are to reduce the number of people who fall ill from the virus and those who die from it. To this end, we suggested a Susceptible–Exposed–Infectious–Recovered (SEIR) type dynamic transmission model of SARS-CoV-2 to explore and analyze the efficacy of public health awareness campaigns in lowering the parthenogenesis of SARS-CoV-2.

In this investigation, we looked at the ABC model for COVID-19 strains. One of the deadliest and most concerning diseases of our day is COVID-19. Infection with the COVID-19 pandemic might be fatal within a matter of weeks due to the severity of its effects. Therefore, greater research into the dynamics of this fragile virus is necessary. Researchers have shown that fractional operators perform well when modeling the spread of infectious diseases. This has sparked a discussion about how the model came to be, whether it exists or is unique, and whether it can be tested for stability using the fixed point theorem. The best-fit curve is based on simulations of the ABC model based on actual cases and cumulative cases on a daily basis, and the fitted parameters are generated from the actual COVID-19 pandemic in Nigeria from March 29 to June 12, 2020, using the least-squares technique. The data sets for this country were selected at random, and any data set can be used to test the validity of the proposed ABC model.

The key epidemiological and theoretical findings of our research work are summarized as follows:

(i) In this research study, the real cases for the pandemic COVID-19 are used to compare the simulations of the proposed model with the ABC operator. The results obtained are in the favor of the fractional operator.
(ii) It has been shown that how the basic reproductive number behaves under the influence of the ABC fractional operator. Thus, it is concluded that the ABC operator provides a better measurement for this threshold quantity.
(iii) Several biological parameters are kept on variation to observe the transmission dynamics of the disease investigated under the ABC operator.
(iv) There are a few existing research studies in the literature to show effectiveness of the ABC models. In this research study, it is found that the ABC operator performs better than its classical version when it comes to the validation of the model. It is done in this study with the help of least-squares curve fitting technique wherein the minimum residual has been computed when the ABC operator comes into effect.
(v) Overall, the ABC operator is found to have better simulation results in comparison to the time-derivative operator taken in the classical sense.

ORCID

Z. U. A. Zafar https://orcid.org/0000-0002-5932-3248
A. Yusuf https://orcid.org/0000-0002-8308-7943
S. S. Musa https://orcid.org/0000-0001-6335-2335
S. Qureshi https://orcid.org/0000-0002-7225-2309
A. S. Alshomrani https://orcid.org/0000-0001-9222-8915
D. Baleanu https://orcid.org/0000-0002-0286-7244

Fractals 2023.31. Downloaded from www.worldscientific.com
by CANKAYA UNIVERSITY on 06/04/24. Re-use and distribution is strictly not permitted, except for Open Access articles.

REFERENCES

1. Q. Li *et al.*, Early transmission dynamics in Wuhan, China, of novel coronavirus-infected pneumonia, *New Engl. J. Med.* **382** (2020) 1199–1207, doi:10.1056/NEJMoa2001316.
2. P. Wu *et al.*, Real-time tentative assessment of the epidemiological characteristics of novel coronavirus infections in Wuhan, China, as at 22 January 2020, *Eurosurveillance* **25**(3) (2020) 2000044.
3. B. Hu, H. Guo, P. Zhou and Z.-L. Shi, Characteristics of SARS-CoV-2 and COVID-19, *Nat. Rev. Microbiol.* **19**(3) (2021) 141–154.
4. WHO, Coronavirus (COVID-19) Dashboard (2021), https://covid19.who.int/ (accessed on 28 July 2021).
5. C. Yang, X. Wang, D. Gao and J. Wang, Impact of awareness programs on cholera dynamics: Two modeling approaches, *Bull. Math. Biol.* **79**(9) (2017) 2109–2131.
6. A. A. de Souza Santos, D. da Silva Candido, W. M. de Souza, L. Buss, S. L. Li, R. H. Pereira, C. H. Wu, E. C. Sabino and N. R. Faria, Dataset on SARS-CoV-2 non-pharmaceutical interventions in Brazilian municipalities, *Sci. Data* **8**(1) (2021) 73.
7. H. Tian *et al.*, An investigation of transmission control measures during the first 50 days of the COVID-19 epidemic in China, *Science* **368** (2020) 638–642.
8. WHO, COVID-2019 vaccines (2021), https://www.who.int/emergencies/diseases/novel-coronavirus-2019/covid-19-vaccines (accessed on 28 July 2021).
9. N. Ferguson, D. Laydon, G. Nedjati-Gilani, N. Imai, K. Ainslie, M. Baguelin, S. Bhatia, A. Boonyasiri, Z. Cucunub, G. Cuomo-Dannenburg and A. Dighe, Report 9: Impact of non-pharmaceutical interventions (NPIs) to reduce COVID19 mortality and healthcare demand, Imperial College London (2020), http://hdl.handle.net/10044/1/77482.
10. Y. Liu, C. Morgenstern, J. Kelly, R. Lowe and M. Jit, The impact of non-pharmaceutical interventions on SARS-CoV-2 transmission across 130 countries and territories, *BMC Med.* **19**(1) (2021) 40.
11. J. Einarsdttir, A. Passa and G. Gunnlaugsson, Health education and cholera in rural Guinea–Bissau, *Int. J. Infect. Dis.* **5**(3) (2001) 133–138.
12. L. F. Buss, C. A. Prete, C. M. Abrahim, A. Mendrone, T. Salomon, C. de Almeida-Neto, R. F. Frana, M. C. Belotti, M. P. Carvalho, A. G. Costa and M. A. Crispim, Three-quarters attack rate of SARS-CoV-2 in the Brazilian Amazon during a largely unmitigated epidemic, *Science* **371**(6526) (2021) 288–292.
13. X. Tang, S. S. Musa, S. Zhao and D. He, Reinfection or reactivation of severe acute respiratory syndrome coronavirus 2: A systematic review, *Front. Public Health* **9** (2021) 663045.
14. Q. Shi, Y. Hu, B. Peng, X. J. Tang, W. Wang, K. Su, C. Luo, B. Wu, F. Zhang, Y. Zhang and B. Anderson, Effective control of SARS-CoV-2 transmission in Wanzhou, China, *Nat. Med.* **27**(1) (2021) 86–93.
15. A. B. Gumel, E. A. Iboi, C. N. Ngonghala and G. A. Ngwa, Toward achieving a vaccine-derived herd immunity threshold for COVID-19 in the US, *Front. Public Health* **9** (2021) 709369, doi:10.3389/fpubh.2021.709369.
16. N. Desai, A. Neyaz, A. Szabolcs, A. R. Shih, J. H. Chen, V. Thapar, L. T. Nieman, A. Solovyov, A. Mehta, D. J. Lieb and A. S. Kulkarni, Temporal and spatial heterogeneity of host response to SARS-CoV-2 pulmonary infection, *Nat. Commun.* **11**(1) (2020) 6319.
17. X. Tang, S. S. Musa, S. Zhao, S. Mei and D. He, Using proper mean generation intervals in modeling of COVID-19, *Front. Public Health* **9** (2021) 691262.
18. J. Tao, X. Zhang, S. S. Musa, L. Yang and D. He, High infection fatality rate among elderly and risk factors associated with infection fatality rate and asymptomatic infections of COVID-19 cases in Hong Kong, *Front. Med.* **8** (2021) 678347.
19. S. S. Musa, S. S. Qureshi, S. Zhao, A. Yusuf, U. T. Mustapha and D. He, Mathematical modeling of COVID-19 epidemic with effect of awareness programs, *Infect. Dis. Model.* **6** (2021) 448–460.
20. A. Atangana, Fractal-fractional differentiation and integration: Connecting fractal calculus and fractional calculus to predict complex system, *Chaos Solitons Fractals* **102** (2017) 396–406.
21. A. Atangana and S. Qureshi, Modeling attractors of chaotic dynamical systems with fractal-fractional operators, *Chaos Solitons Fractals* **123** (2019) 320–337.
22. K. A. Abro and A. Atangana, Numerical and mathematical analysis of induction motor by means of AB–fractal–fractional differentiation actuated by drilling system, *Numer. Methods Partial Differential Equations* **38**(3) (2022) 293–307.
23. P. A. Naik, M. Yavuz, S. Qureshi, J. Zu and S. Townley, Modeling and analysis of COVID-19 epidemics with treatment in fractional derivatives using real data from Pakistan, *Eur. Phys. J. Plus* **135**(10) (2020) 795.
24. D. Baleanu, H. Mohammadi and S. Rezapour, A fractional differential equation model for the COVID-19 transmission by using the Caputo–Fabrizio derivative, *Adv. Differ. Equ.* **2020**(1) (2020) 299.
25. I. Ahmed, I. A. Baba, A. Yusuf, P. Kumam and W. Kumam, Analysis of Caputo fractional-order model for COVID-19 with lockdown, *Adv. Differ. Equ.* **2020**(1) (2020) 394.

26. R. Zarin, A. Khan, A. Yusuf, S. Abdel-Khalek and M. Inc, Analysis of fractional COVID-19 epidemic model under Caputo operator, *Math. Methods Appl. Sci.* **46**(7) (2023) 7944–7964.
27. D. Baleanu, A. Jajarmi, E. Bonyah and M. Hajipour, New aspects of poor nutrition in the life cycle within the fractional calculus, *Adv. Differ. Equ.* **2018** (2018) 230, doi:10.1186/s13662-018-1684-x.
28. F. M. Khan, Z. U. Khan, Y.-P. Lv, A. Yusuf and A. Din, Investigating of fractional order dengue epidemic model with ABC operator, *Results Phys.* **24** (2021) 104075, doi:10.1016/j.rinp.2021.104075.
29. S. Qureshi and R. Jan, Modeling of measles epidemic with optimized fractional order under Caputo differential operator, *Chaos Solitons Fractals* **145** (2021) 110766, doi:10.1016/j.chaos.2021.110766.
30. Nigeria Centre for Disease Control (NCDC), Coronavirus disease (COVID-19), situation reports (2020), https://covid19.ncdc.gov.ng/.
31. S. S. Musa, S. Zhao, M. H. Wang, A. G. Habib, U. T. Mustapha and D. He, Estimation of exponential growth rate and basic reproduction number of the coronavirus disease 2019 (COVID-19) in Africa, *Infect. Dis. Poverty* **9** (2020) 96, doi:10.1186/s40249-020-00718-y.
32. S. S. Musa, D. Gao, S. Zhao, L. Yang, Y. Lou and D. He, Mechanistic modeling of the coronavirus disease 2019 (COVID-19) outbreak in the early phase in Wuhan, China, with different quarantine measures, *Acta Math. Appl. Sin.* **43**(2) (2020) 350–364.
33. B. Tang, X. Wang, Q. Li, N. L. Bragazzi, S. Tang, Y. Xiao and J. Wu, Estimation of the transmission risk of the 2019-nCoV and its implication for public health interventions, *J. Clin. Med.* **9** (2020) 462, doi:10.3390/jcm9020462.
34. B. S. T. Alkahtani, A. Atangana and I. Koca, Novel analysis of the fractional Zika model using the Adams type predictor–corrector rule for non-singular and non-local fractional operators, *J. Nonlinear Sci. Appl.* **10**(6) (2017) 3191–3200.
35. N. Chitnis, J. M. Hymann and J. M. Cushing, Determining important parameters in the spread of Malaria through the sensitivity analysis of a mathematical model, *Bull. Math. Biol.* **70**(5) (2008) 1272–1296.

Fractals 2023.31. Downloaded from www.worldscientific.com
by CANKAYA UNIVERSITY on 06/04/24. Re-use and distribution is strictly not permitted, except for Open Access articles.